A TGA study of tobacco combustion assuming DAEM devolatilization and empirical char burn-off kinetics

Gábor Várhegyi,[†,] Zsuzsanna Czégény,[†] Chuan Liu[‡] and Kevin McAdam[‡]*

[†] Institute of Materials and Environmental Chemistry, Chemical Research Center, Hungarian Academy of Sciences, P.O. Box 17, Budapest 1525, Hungary; and [‡] *GR&D, British American Tobacco, Regents Park Road, Southampton SO15 8TL, United Kingdom.*

[*] To whom correspondence should be addressed.
Email: varhegyi.gabor@t-online.hu or gvarhegyi@gmail.com

ABSTRACT. Two blends of tobacco (Virginia and Burley) were studied by thermogravimetry at linear and nonlinear heating programs in gas flows containing 2, 4 and 9% oxygen. A kinetic scheme of successive devolatilization and char burn-off reactions was assumed. A distributed activation energy model was assumed for the devolatilization with a Gaussian distribution and a constant pre-exponential factor. The evaluations were also carried out using non-constant pre-exponential factors that depended on the activation energy. The char burn-off was described by first order kinetics and by an empirical model that took into account the change of the reactivity with the conversion of the sample. The dependence of the rate of combustion on the oxygen concentration was approximated by a power function. Series of 15 and 30 experiments were used for the determination of the model parameters by simultaneous least squares evaluation of the experiments. The considerations, methods and results can also be used in the field of biomass gasification and combustion.

Keywords: Tobacco blends; biomass; thermogravimetry; distributed activation energy model; combustion; pyrolysis; kinetic regime.

1. Introduction

The primary goal of this work was to develop kinetic submodels describing the pyrolysis and combustion processes occurring during the burning of tobacco. As the reactions studied in our work also occur in the combustion of other plant materials and solid biomass fuels the considerations, methods, models, algorithms and results of our work are also expected to be applicable to research into biomass gasification and combustion in general.

Thermogravimetric experiments have a high precision as the temperature and the other experimental conditions of the sample are usually well known and well controlled. This makes it a useful tool for studying devolatilization and combustion in the kinetic regime.[1,2] On the other hand, TGA can be employed only at relatively low heating rates; at high heating rates the true temperature of the sample may be unknown. This is particularly true in the presence of oxygen when high heating rates and/or larger sample masses can lead to ignition and uncontrolled combustion of the sample.

TGA measures the overall mass loss caused by devolatilization and burn-off of the formed char. These processes more or less overlap each other; accordingly their evaluation needs a suitable kinetic model that considers the simultaneous occurrence of both processes.[3] The development of this type of model was the main subject of the present work.

Most materials and products made from plants contain a wide variety of pyrolyzing species. Even the same chemical species may have differing reactivity if their pyrolysis is influenced by other species in their vicinity. The assumption of a distribution in the reactivity of the decomposing species frequently helps in the kinetic evaluation of the pyrolysis of complex organic samples.[4] The distributed activation energy models (DAEM) have been used for biomass pyrolysis kinetics since 1985, when Avni et al. applied a DAEM for the formation of volatiles from lignin.[5] This type of research was subsequently extended to a wider range of biomasses and materials derived from plants including several works on tobacco devolatilization.[6-9] Saidi et al. employed a DAEM in an actual combustion model.[10] Becidian et al.[11] described the pyrolysis of wastes from brewery, industrial coffee roasting, and fiberboard furniture production by DAEM kinetics. This work used the method of least squares on series of experiments with linear and non-linear temperature programs in a similar way as it is employed in the present work. The model parameters obtained by Becidian at al. allowed reliable prediction outside of the domain of the experimental conditions of the given kinetic evaluations. Recently Várhegyi et al. employed a similar kinetic evaluation on large series of experimental data in a TGA-MS study of tobacco pyrolysis in inert atmosphere.[12]

There are many papers dealing with the gasification and burn-off kinetics of lignocellulosic chars. This part of the literature has recently been extensively reviewed by Di Blasi.[13] The paper of Várhegyi et al. on the combustion kinetics of corn cob charcoals[14] has close relationships to the present paper due to similarities in the least squares evaluation strategies and the application of an empirical model.

A combustion model usually needs the coupling of the devolatilization and the char burn-off reactions.[15] The present work deals with the devolatilization and successive char-burn-off that occur in overlapping time/temperature intervals. Four model variations were tested by determining the model parameters and

verifying the models on large series of experiments using the method of least squares. The present work differs from its predecessors[11,12,14] in the model variants employed as well as in the coupling of a DAEM devolatilization with char burn-off kinetics.

2. Samples and Methods

2.1. Samples. Virginia and Burley tobaccos are the two tobacco varieties that are present in the largest quantities in most commercial tobacco products. Different growing and curing conditions have led to significant differences in their chemical compositions. Virginia-style and Burley-style tobacco blends were investigated in the present work. The Virginia sample consisted of eight different tobaccos (laminar grades) from eight different countries, each making 12.5 m/m%. The Burley sample was blended from four different tobaccos (laminar grades) grown in four countries.

Table 1. Characteristics of the Virginia and Burley tobacco blends

m/m % on a dry weight basis	Virginia	Burley
Ash	11.9	20.3
Total nitrogen	2.7	4.7
Total sugars	13.2	0.1
Pectins	6.9	9.9
Cellulose	10.2	13.0
Lignin	3.7	4.2
Nicotine	2.8	2.6
Polyphenols (chlorogenic acid + rutin)	2.6	0.1

The main chemical characteristics of the samples are summarized in Table 1. It is interesting to note that these tobacco blends contain more minerals then a usual biomass fuel; the ash content of the Virginia and Burley blends were 12 and 20 %, respectively. The composition of the ash is similar in the two tobaccos, as shown by an ICP-OES spectrometry analysis in Table 2. The pyrolysis of these samples was studied in two recent works published elsewhere. Czégény et al. studied the formation of selected toxicants by pyrolysis – gas chromatography – mass spectrometry and presented TGA experiments about the effect of sample mass, particle size and oxygen concentration.[16] Várhegyi et al. examined the pyrolysis kinetics of these samples in inert atmosphere by TGA-MS experiments.[12] (See Section 3.6 for data from the latter work.)

The tobacco samples for the experiments were taken from research cigarettes. The tobacco was slightly broken in an agate mortar, mixed, and put into a closed jar at room temperature. For each experiment a small amount of tobacco was sourced out from the jar. The moisture content of the Virginia and Burley tobacco samples were found to be 4.8 and 4.9 m/m% before the experiments, respectively. These values are lower than

the moisture content was in the original cigarettes. However, the moisture content has no effect on the kinetics of the TGA studies because the samples in thin layers dry before reaching the temperatures of the pyrolysis and combustion reactions.

Table 2. Ash analysis[a]

m/m %	Virginia	Burley
Al	0.7	0.6
Ca	21.5	18.7
Fe	0.3	0.3
K	30.2	28.2
Mg	5.2	3.8
Na	0.4	0.4

[a] The ash was prepared by CEN/TS 14775 standard. The concentrations are expressed on a dry weight basis. The analysis was carried out on 19 elements of which the metallic components with concentration above 0.1% are shown.

2.2. Thermogravimetric experiments. The TGA measurements were performed using a computerized Perkin-Elmer TGS-2 thermobalance. Samples of 0.4 - 2 mg were spread on a platinum sample holder of Ø 6 mm. The experiments were carried out in gas flows of 140 ml/min. Nitrogen – oxygen mixtures with 2, 4 and 9 % (v/v, ±5% rel.) oxygen were used. Prior to the experiments, the apparatus was purged with the carrier gas for 45 min. Linear and stepwise heating programs were employed to increase the amount of information in the series of experiments.[17] As Figure 1 shows, the heating programs slightly differed for the two samples due to differences in the domain of devolatilization and in the reactivity of the chars. Test experiments were carried out to select sample masses at which no ignition or significant self-heating occurred. Self heating can be a serious problem in combustion studies, as illustrated in earlier works.[14,17] At a heating rate of 40°C/min the safe sample mass proved to be around 0.4 mg in the present work. However, a sample mass of 0.4 mg contained only 2-3 tobacco pieces. This resulted in some sample-to-sample variation of these experiments that can be seen in the corresponding figures of the *Supporting Information*. Accordingly, each 40°C/min experiment was conducted in duplicate. In this way 6 experiments of 40°C/min were used for each sample in the kinetic evaluation. 1 mg sample mass was employed at the T(t) denoted by bold solid lines in Figure 1 while 2 mg sample could safely be used at the slower heating programs (circles and dashed lines in Figure 1).
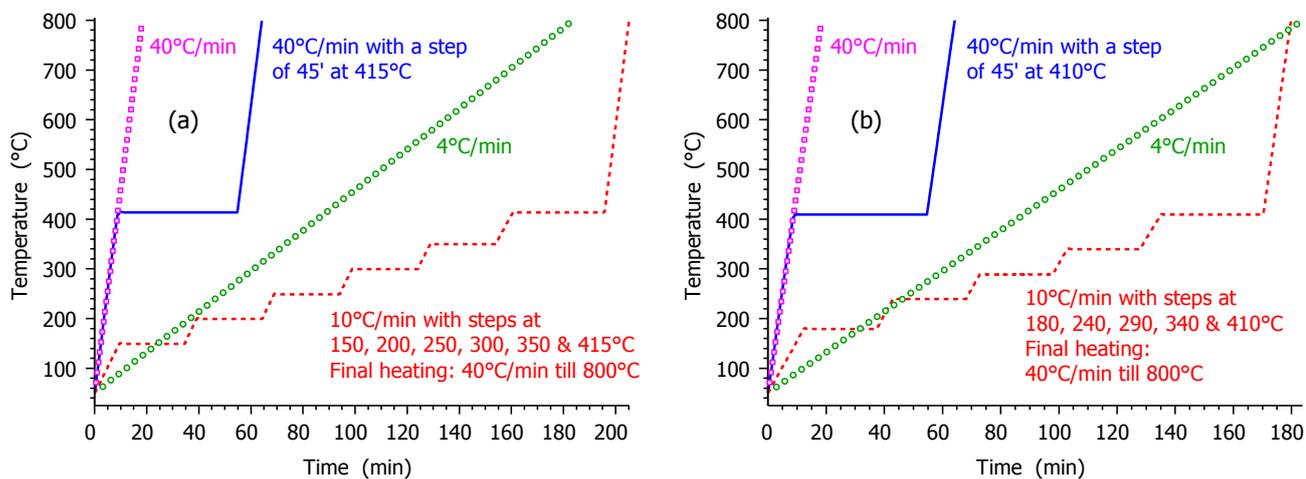
Figure 1. Heating programs for the Virginia (a) and the Burley (b) samples.

2.3. Numerical methods. The calculations were carried out on personal computers running Windows. The calculation rates given in this work were determined using an Intel Core 2 Quad Q9550 processor running at 2.8 GHz. The parallel processing capabilities of this processor were not used in the programming. Fortran 95 and C++ were employed for the numerical calculations and for graphics handling, respectively. Earlier programs developed and employed by one of the authors[11,14,17-20] were supplemented in the present work by a fast algorithm for the solution of the coupled DAEM devolatilization and char combustion reactions. The algorithms used are briefly summarized below, incorporating some essential details that were omitted in our earlier works.

The derivative of the sample mass curves (DTG) were determined by the analytical differentiation of smoothing splines, as described by Várhegyi and Till.[19] The rms difference between the spline function and the measured TGA data was around 0.16 µg, which is negligible compared to the initial sample masses of this work (0.4 – 2 mg). This procedure does not introduce considerable systematic errors into the least squares kinetic evaluation of experimental results.[20] The differential equations of the model were solved numerically along the empirical temperature – time functions resulting in simulated data in the t_i points of the observations. As outlined in the next section, a DAEM devolatilization and a subsequent char burn-off reaction were assumed. The integration by E in the DAEM kinetics was carried out by a Gauss - Hermite quadrature formula, as described by Donskoi and McElwain[21] and Várhegyi et al.[18] The domain of integration was rescaled by a factor of 0.2 to increase the precision of the integration.[21] The first order kinetic equations of the DAEM were solved numerically using 180 quadrature points. Obviously the solution of the kinetic equations is not needed in the lower part of the activation energy range. This can be easily checked: if the rate constant ($A_0 e^{-E/RT}$) is higher than 10^3 s^{-1} in the first evaluated point of the domain of evaluation, then the mean lifetime of the corresponding species is less than a millisecond there. (In a more general sense, the actual activation energy limit should obviously be set to the time scale and precision requirements of the given work.) A limit can also be implemented in the solution of the first order kinetic equations: the integration can obviously be finished if the normalized amount of the given species reaches a low value, e.g. 10^{-12}. A similar limit can be set at the high end of the E domain, too, by calculating the rate constant at the highest evaluated temperature. If

5

its reciprocal is much higher than the time scale of the problem then only a negligible part of the corresponding species will decompose and the kinetic equation need not be solved at this E.

After separating the variables in the first order kinetic equations, the exponential integral was solved numerically in each $[t_{i-1}, t_i]$ by a Gauss – Legendre quadrature of 7 points of which the first and last were fixed to be at the end points of the given $[t_{i-1}, t_i]$ domain.[22] This procedure works at any T(t) function that may arise in thermal analysis. A linear T(t) was assumed at the beginning of the integration, from room temperature to the first point of the evaluation, accordingly it is possible to use an analytical approximation of the exponential integral in these intervals. Legendre's continued fractions were used in this work, as described earlier.[23] The solution of the DAEM gave the amount of unreacted sample, $m_{ur}(t)$ and its derivative, dm_{ur}/dt in the t_i points. (See the notations in the *Nomenclature* at the end of the paper.) The solution of the char burn-off equation required the $m_{ur}(t)$ and dm_{ur}/dt at many other t values. These data were obtained from the discrete $m_{ur}(t_i)$ and $\frac{dm_{ur}}{dt}(t_i)$ values by Hermitian interpolation. The differential equation of the char burn-off kinetics was solved by an adaptive stepwise Runge–Kutta method[24] in each $[t_{i-1}, t_i]$ interval. To simplify the programming, the equations for the overall mass and for the ash production were also solved together with the char burn-off equation in the same Runge–Kutta calculations. The nonlinear least squares minimization was carried out by a variant of the Hook–Jeeves method, which is a slow but simple and dependable direct search algorithm.[25] In our work the original Hook–Jeeves algorithm was supplemented by parabolic interpolation for finding the optimal stepsizes. The starting values for the non-linear optimization were taken either from earlier work[11,14] or from the results of the simpler models of the present work.

3. Results and discussion

3.1. Evaluation by the method of least squares. The unknown model parameters were evaluated from series of experiments by minimizing sum S_N:
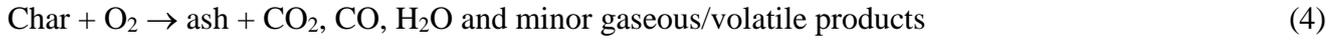
$$S_N = \sum_{k=1}^{N} \frac{w_k}{W} \sum_{i=1}^{N_k} \frac{\left[\left(\frac{dm}{dt}\right)_k^{obs}(t_i) - \left(\frac{dm}{dt}\right)_k^{calc}(t_i)\right]^2}{N_k h_k^2} \tag{1}$$

Here N is the number of experiments in the series. In the present work its value is either 15 or 30. The w_k weight factors were 0.5 for the 40°C/min experiments (of which we had duplicates in the least squares sum, as described in Section 2.2) and 1 for the other experiments. W is the sum of w_k. $(dm/dt)^{obs}$ and $(dm/dt)^{calc}$ denote the observations and their simulated counterparts. Subscript k indicates the different experiments. t_i denotes the time values in which the discrete experimental values were taken, and N_k is the number of the t_i points in a given experiment. h_k denotes the heights of the evaluated curves that strongly depend on the experimental conditions. The division by h_k^2 serves for normalization. The fit was characterized by the following quantity:

$$fit_N\,(\%) = 100\ S_N^{0.5} \tag{2}$$

6

Equations 1 and 2 can be employed to express the fit of any group within the evaluated experiments. When the fit is calculated for one experiment, $S_1^{0.5}$ equals to the normalized rms deviation of the calculated data from the observations.

3.2. Coupling a DAEM devolatilization and a successive char burn-off reaction. The following successive reactions will be considered:

Tobacco $\rightarrow$ char + volatiles $\qquad\qquad$ (3)

Char + O_2 $\rightarrow$ ash + CO_2, CO, H_2O and minor gaseous/volatile products $\qquad\qquad$ (4)

Let us normalize all masses by the initial sample mass. The normalized amounts of the unreacted part of the sample, char and ash will be denoted by m_{ur} and m_{char}, and m_{ash}, respectively.

As the reactions proceed, m_{ur} decreases from 1 to 0. m_{char} is zero at the beginning of an experiment. It reaches a maximum as the char forms and converges to zero again as the char burns off. The yields of the solid products in reactions 3 and 4 will be denoted by y_{char} and y_{ash}, respectively. As the char burn-off proceeds, m_{ash} converges from 0 to $y_{char} y_{ash}$.

m^{calc} is the sum of the normalized masses of the solid components:

$m^{calc} = m_{ur} + m_{char} + m_{ash}$ $\qquad\qquad$ (5)

$dm^{calc}/dt = m_{ur}/dt + m_{char}/dt + m_{ash}/dt$ $\qquad\qquad$ (6)

Note that $m^{calc}(0)=1$ and $m^{calc} \rightarrow y_{char} y_{ash}$ as $t \rightarrow \infty$.

The devolatilization is described by a DAEM. First order reactions are assumed for the parts of the sample that decompose at the various E values:

$-dm_{ur}(t,E)/dt = A_0\, e^{-E/RT}\, m_{ur}(t,E)$ $\qquad\qquad$ (7)

$m_{ur}(t)$ is composed from $m_{ur}(t,E)$:

$$m_{ur}(t) = \int_0^\infty D(E)\, m_{ur}(t,E)\, dE \qquad\qquad (8)$$

$D(E)$ will be approximated by a Gaussian distribution:

$D(E) = (2\pi)^{-1/2}\, \sigma^{-1} \exp[-(E-E_0)^2/2\sigma^2]$ $\qquad\qquad$ (9)

In this section the char burn-off is approximated by a simple kinetic relationship which is first order with respect to the amount of char and v^{th} order with respect to the oxygen concentration:

$dm_{char}/dt = dm_{ur}/dt\; y_{char} - A_{char} \exp(-E_{char}/RT)\, m_{char}\, C_{O_2}^{v}$ $\qquad\qquad$ (10)

Here C_{O_2} is the dimensionless V/V concentration of the oxygen. (Note that a dimensionless C_{O_2} is necessary to provide a constant dimension for A_{char}, which is s^{-1} in this way.)

The ash is formed from the char burn-off with yield y_{ash} and does not react any further in this model:

$dm_{ash}/dt = A_{char} \exp(-E_{char}/RT)\, m_{char}\, C_{O_2}^{v}\, y_{ash}$ $\qquad\qquad$ (11)

The solution of equations 5 – 11 was carried out numerically, as described in Section 2.3. A high relative precision was used (better then 10^{-6}) because it ensured the safety of the iterations and did not cause any

difficulty. The average time of solution of equations 5 – 11 at a given $T(t)$ was 29 ms by the computer described in Section 2.3.

3.3. Simultaneous evaluation of 15 and 30 experiments. First the 15 experiments of a given tobacco blend was evaluated by this model. The means of the activation energy distribution, E_0 and the activation energies of the char burn-off, E_{char} showed only slight variations with the tobacco blends. The corresponding parameters are presented in Table 3, under the headings "DAEM: Constant A" and "char burn-off: 1st order with respect to m_{char}". It was found that common ν reaction orders can be selected for the two blends without a significant worsening of the fit. Accordingly, the 30 experiments of the two tobacco blends could be evaluated together assuming common values for E_0, E_{char}, and ν. As the corresponding part of Table 4 shows, this procedure resulted in practically the same fit_{30} values as the separate evaluation of the samples. In this case 13 unknown parameters were determined from 30 experiments, indicating a good mathematical condition of the evaluation. The details of the evaluation are displayed in Figure 2. Red color indicates the conversion of the unreacted sample, blue color shows the formation and burn-off of the char and green color represents the ash production. (Note that the negative parts of the figures indicate the formation of the products in this representation.)

Table 3. Parameters obtained from two series of 15 experiments at all model variants employed

| DAEM	Constant A		A depends on E		Constant A		A depends on E	
Char burn-off	1st order with respect to m_{char}				Empirical dependence on α and m_{char}			
Sample	Virginia	Burley	Virginia	Burley	Virginia	Burley	Virginia	Burley
fit_{15} (%)	8.5	6.8	8.2	6.7	8.1	6.0	7.7	5.9
fit_{30} (%)	7.7		7.5		7.1		6.9	
$\beta\,/\,kJ^{-1}\,mol$	–	–	0.113	0.085	–	–	0.106	0.065
$E_0\,/\,kJ\,mol^{-1}$	180	185	169	184	184	188	170	186
$\sigma\,/\,kJ\,mol^{-1}$	25.8	17.3	51.1	28.0	26.4	18.0	52.5	25.3
$\log_{10} A_0\,/\,s^{-1}$	14.88	15.17	14.22	15.08	15.28	15.39	14.28	15.24
y_{char}	0.42	0.54	0.41	0.54	0.42	0.53	0.40	0.53
$E_{char}\,/\,kJ\,mol^{-1}$	204	215	201	214	210	216	210	216
$\log_{10} A_{char}/s^{-1}$	13.02	13.74	12.74	13.67	14.20	14.40	14.09	14.00
ν	0.54	0.32	0.51	0.32	0.56	0.34	0.53	0.34
y_{ash}	0.31	0.49	0.23	0.48	0.29	0.47	0.18	0.46
n	–	–	–	–	1.76	2.17	1.71	2.13
a	–	–	–	–	2.60	5.42	1.99	5.89
z	–	–	–	–	0.00	0.23	0.00	0.39

Table 4. Parameters obtained from a series of 30 experiments at all model variants employed

DAEM	Constant A		A depends on E		Constant A		A depends on E	
Char burn-off	1st order with respect to m_{char}				Empirical dependence on α and m_{char}			
Sample	Virginia	Burley	Virginia	Burley	Virginia	Burley	Virginia	Burley
fit_{30} (%)	7.8		7.6		7.2		7.0	
fit_{30} (%), T≤400°C[a]	6.4		5.4		6.4		5.5	
fit_{30} (%), T>400°C[a]	11.0		11.2		9.8		9.9	
β / kJ⁻¹ mol	–		0.107	0.089	–		0.106	0.071
E_0 / kJ mol⁻¹	186		180		186		182	
σ / kJ mol⁻¹	26.7	17.2	51.4	28.3	26.7	17.7	52.8	25.4
$\log_{10} A_0$ / s⁻¹	15.43	15.18	15.24	14.76	15.43	15.17	15.37	14.86
y_{char}	0.42	0.54	0.41	0.54	0.42	0.53	0.40	0.54
E_{char} / kJ mol⁻¹	211		209		213		212	
$\log_{10} A_{char}$/s⁻¹	13.31	13.57	13.16	13.41	14.38	14.54	14.32	14.45
ν	0.42		0.41		0.43		0.42	
y_{ash}	0.32	0.49	0.25	0.48	0.29	0.47	0.20	0.46
n	–		–		1.96		1.92	
a	–		–		3.42		3.09	
z	–		–		0.01		0.01	

[a] Separate fit_{30} values were calculated for the experimental points below and above 400°C to show how the models fit the data in domains dominated by devolatilization and char burn-off, respectively.
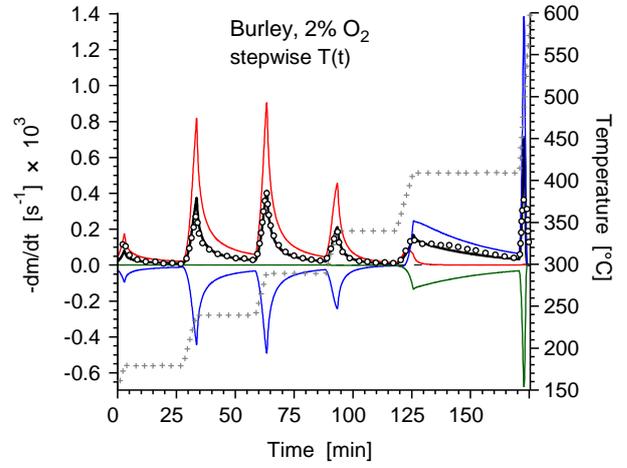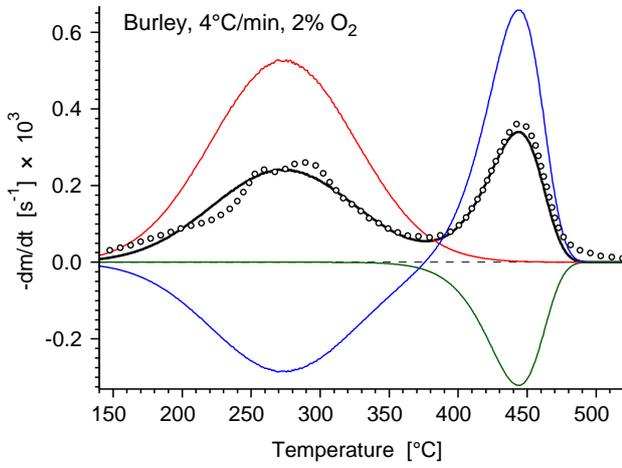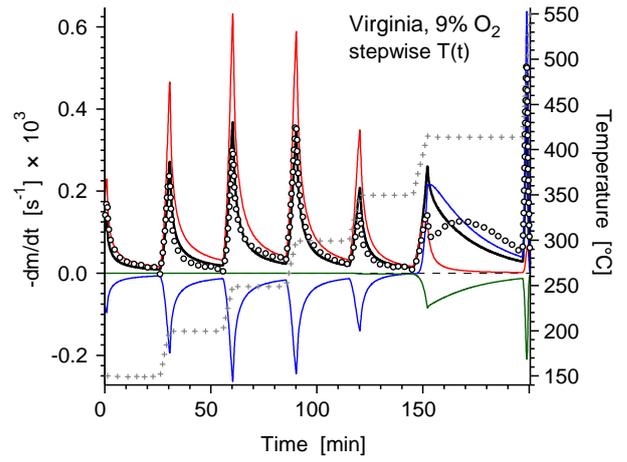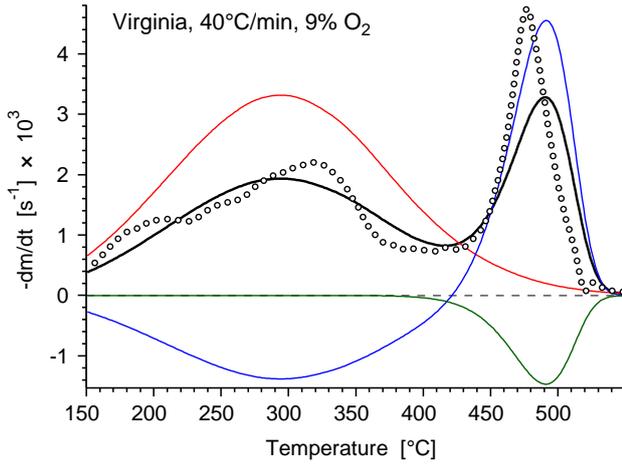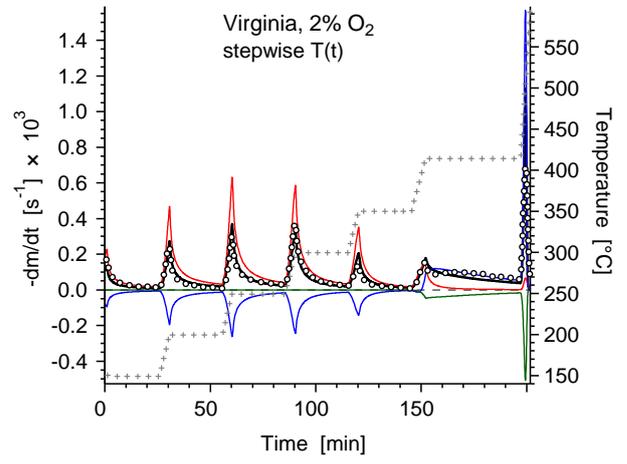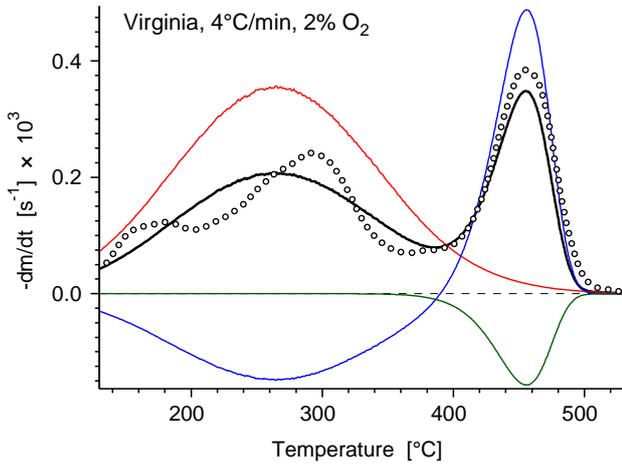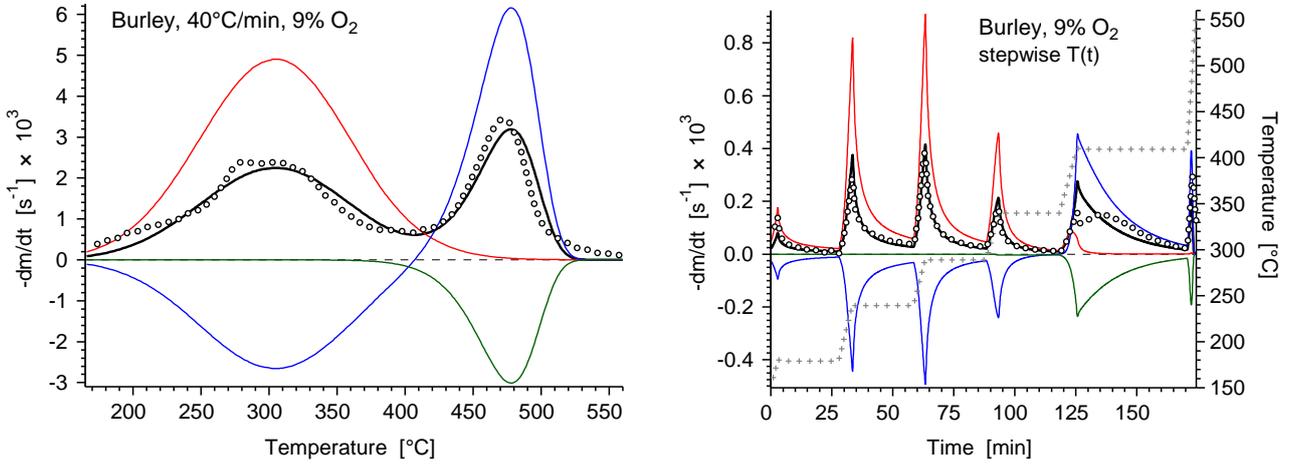
Figure 2. Simultaneous evaluation of 30 experiments as described in Sections 3.2 and 3.3. Model assumptions: constant pre-exponential factor in the DAEM devolatilization and first order char burn-off kinetics with respect to m_{char}. Eight experiments are shown here, the rest can be found in the *Supporting Information*. Notation: experimental DTG curves normalized by the initial sample mass (∘∘∘); their calculated counterpart (black ▬); and simulated partial curves -dm_{ur}/dt (red —); -dm_{char}/dt (blue —); and -dm_{ash}/dt (green —). The stepwise temperature programs (+ + +) are also shown when appropriate.

3.4. An empirical char burn-off model. In the case of ideal chars (specially prepared, pure model carbons) the reaction rate is proportional to the surface area, and the change of the surface area during the reaction can be described by theoretical models.[26-29]. In the case of a tobacco or a biomass fuel, however, complicating factors arise that are connected to the accessibility of the internal pores, the role of the inorganic catalysts, and the chemical/physical inhomogeneity of the solid phase. These factors hinder the deduction of theoretical models. The use of an appropriate empirical formula with adjustable parameters is more viable.

The following empirical formula has proved useful in describing the burn-off of char samples[14,30]:

$$f(\alpha) = normfactor\ (1-\alpha)^n\ (\alpha+z)^a \tag{12}$$

Here α is the reacted fraction of a char sample, n, a and z are formal parameters determining the shape of $f(\alpha)$ and *normfactor* normalizes the maximum of eq 12 to unity. A wide variety of functions can be described by this formula that differ in shape, symmetry, and peak position.[31]

Eq 12 was modified for the present case when the tobacco char forms during the devolatilization. In such cases the formation, growing and accessibility of the pores will be affected by the overall conversion of the sample. Let us denote the reacted fraction of the sample by α:

$$\alpha(t) = \frac{m^{calc}(t) - m^{calc}(\infty)}{m^{calc}(0) - m^{calc}(\infty)} = \frac{m^{calc}(t) - y_{char}y_{ash}}{1 - y_{char}y_{ash}} \tag{13}$$

The equations for char burn-off and ash formation will be written in the form

$$dm_{char}/dt = dm_{ur}/dt\ y_{char} - A_{char}\ \exp(-E_{char}/RT)\ f(\alpha, m_{char})\ C_{O_2}^v \tag{14}$$

$$dm_{ash}/dt = A_{char}\ \exp(-E_{char}/RT)\ f(\alpha, m_{char})\ C_{O_2}^v\ y_{ash} \tag{15}$$

12

where $f(\alpha,m_{char})$ is the function expressing the dependence of the char-burn-off rate on α and m_{char}. $f(\alpha,m_{char})$ will be approximated by

$$f(\alpha,m_{char}) = m_{char}^n \, (\alpha+z)^a \qquad (16)$$

where $n>0$, $a\geq0$ and $z\geq0$ are empirical parameters. The first part, m_{char}^n has a monotonous dependence on m_{char} and ensures the zero burn-off rate at $m_{char}=0$. The second part, $(\alpha+z)^a$, expresses that the conversion of the sample may result in growing pores and may enhance the accessibility of the pores, too.

The replacement of equations $10-11$ by $14-16$ increased the average solution time of the model from 29 to 32 ms at a given $T(t)$ on the computer described in Section 2.3. The evaluations carried out with this model resulted in an improvement of the fit, as shown in the corresponding fields of Tables 3 and 4. (See the values under headings "DAEM: Constant A" and "char burn-off: Empirical dependence on α and m_{char}".) Unfortunately no statistical background is available to evaluate the statistical significance of these changes in the *fit* values because the main experimental errors of the thermal analysis are neither random nor independent.[17] The improvement of the fit occurs obviously in the domain dominated by the char burn-off, as the *fit*$_{30}$ values at T>400°C indicate in Table 4. The figures on the evaluation with this model variant can be found in the *Supporting Information*.

It is interesting to have a closer look on the obtained $f(\alpha,m_{char})$ functions since they reveal details on the char burn-off. The ratio of $f(\alpha,m_{char})$ and m_{char} was plotted for this purpose because it shows how the reactivity of a unit amount of char is influenced by the conversion of the sample. In Figure 3 circle and square symbols represent these ratios when the DAEM variant of Section 3.1 was used. The solid and dashed lines belong to a DAEM variant treated in the next section. Panel (a) of Figure 3 shows that similar curves were obtained for the two tobacco samples based on a series of 15 experiments. Panel (b) shows the case when 30 experiments were evaluated and common $f(\alpha,m_{char})$ parameters were assumed for the samples. In the latter case the two DAEM variants of the work gave nearly identical results. Note that the curves in Figure 3 were magnified to an equal height since the kinetic equations do not define physically the height of the $f(\alpha,m_{char})$ functions. (Because the model contains the product of A_{char} and $f(\alpha,m_{char})$.) The curves in Figure 3 express a strong dependence of the char reactivity on the conversion of the sample.
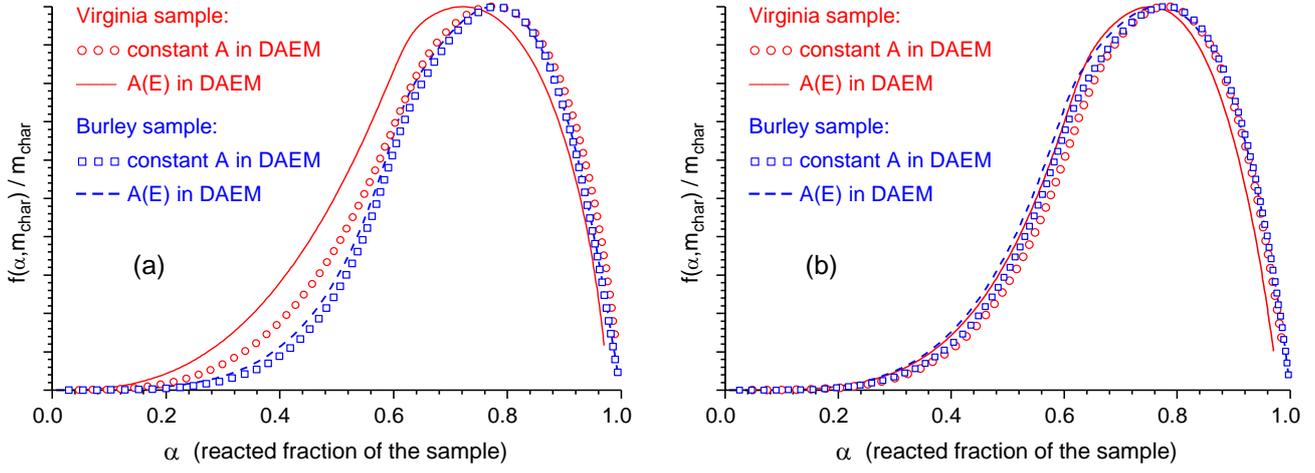
Figure 3. The ratio of $f(\alpha, m_{char})$ and m_{char} obtained from series of 15 experiments (a) and 30 experiments (b). The terms "constant A in DAEM" and "A(E) in DAEM" refers to the DAEM variants outlined in Sections 3.2 and 3.5, respectively.

3.5. DAEM devolatilization with non-constant pre-exponential factor. In 1995 Miura suggested the use of distributed activation energy models with pre-exponential factors that depend on the activation energy.[32] The corresponding evaluation was based on the tabular and graphic representations for the activation energy distribution and the dependence of the pre-exponential factor. Miura's approach has been used in many later works, including a modified evaluation method[33] and a recent work on biomass pyrolysis.[34]

In this section a pre-exponential factor depending on E will be introduced into the model of the present work. The reason behind this extension is that the assumption of a constant A in a wide domain of E looks unrealistic; one should expect some dependence of A on E. We could not follow Miura's method for the tabular determination of $A(E)$ values because our work is based on models that can produce the simulated counterparts of the experimental data via a numerical solution. Accordingly equations built from analytical formulas were considered. An empirical formula was adapted from the work of Miura[32] and Hashimoto et al.[35] that assumes a linear dependence between E and the logarithm of the activation energy:

$$A(E) = const \exp(\beta E) = A_0 \exp[\beta(E-E_0)] \tag{17}$$

where A_0 is the pre-exponential factor value at the mean of the energy distribution, E_0. With a variable A, the first order kinetic equation of the DAEM has the following form:

$$-\mathrm{d}m_{ur}(t,E)/\mathrm{d}t = A(E)\, \mathrm{e}^{-E/RT}\, m_{ur}(t,E) \tag{18}$$

The rest of the equations have not changed and the same algorithms could be used with the same calculation rates as in the previous sections. The results are listed in Tables 3 and 4 under the headings "DAEM: A depends on E".

As the data shows, the overall fit has slightly improved by the introduction of eq 17. The improvement of the fit occurs notably in the domain dominated by the devolatilization, as the fit_{30} values at T≤400°C indicate in Table 4. The differences in these fit values are not high indicating that the $A(E)$ dependence of eq. 17 can be well approximated by a constant activation energy DAEM. Most of the parameters in Tables 3 and 4 varied only slightly by the introduction of the $A(E)$ dependence. The most noticeable exception is the high increase of

14

the σ values. This can easily be explained by considering how β effects the peak position of the first order kinetic equations, as shown in Figure 4. The basis of the comparison is the solution at A_0 and E_0 which is represented by the bold solid line. Thin solid lines show the solutions with the same A_0 pre-exponential factor at lower and higher activation energies. Dashed lines represent the solution if eq 17 is assumed. The corresponding parameter values are listed in the caption of Figure 4. One can see that a positive β narrows the distribution. This narrowing can be compensated by a higher width of the distribution. Any monotonous increase in $A(E)$ dependence would result in some narrowing of the distribution, similar to the example shown. If the effect is nearly symmetric (like in Figure 4) then a higher σ can more or less compensate it.

A closer look on the parameters reveals that the introduction of the $A(E)$ dependence had a greater effect on the parameters of the Virginia tobacco blend. The change of the y_{ash} parameter of the Virginia sample is particularly excessive. We did not analyze the causes of this effect. The changes in the $f(\alpha, m_{char})$ / m_{char} ratios are not particularly high when the evaluation was based on 15 experiments, as Figure 3 shows. The evaluation of the 30 experiments together resulted in nearly identical $f(\alpha, m_{char})$ / m_{char} ratios. Similarly, the differences between the parameters obtained with and without the assumption of the A(E) dependence are smaller in Table 4 than in Table 3. (The only exceptions are the σ vales and the y_{ash} of the Virginia sample.)
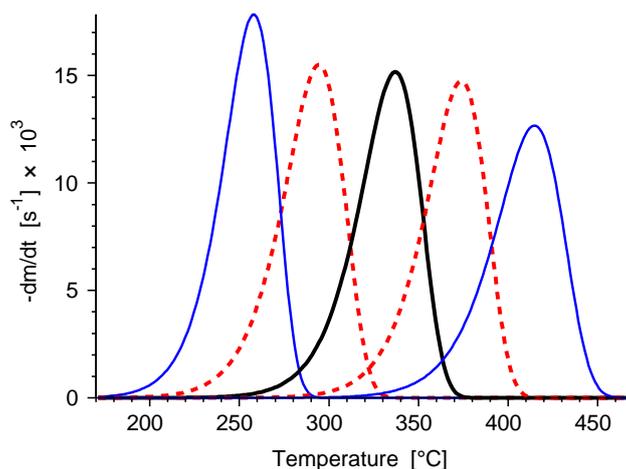
Figure 4. Comparison of first order reactions with and without the assumption of a non-constant pre-exponential factor by eq. 17. Parameters: $E_0 = 180\,\mathrm{kJ\,mol^{-1}}$, $A_0 = 10^{14}\,\mathrm{s^{-1}}$, $\sigma_0 = 24\,\mathrm{kJ^{-1}\,mol}$, β=0.1. Bold solid line (black): $E=E_0$ and $A=A_0$. Thin solid lines (blue): $E=E_0-\sigma$ and $E=E_0+\sigma$ at $A=A_0$. Dashed lines (red): $E=E_0-\sigma$ and $E=E_0+\sigma$ at $A=A(E)$. The curves were simulated at a linear T(t) with dT/dt=40°C/min.

3.6. Notes on the magnitudes of the obtained kinetic parameters. In this paragraph the results will be compared with kinetic parameters from the recent literature. Only the constant pre-exponential factor results of Tables 3 and 4 will be considered due to the compensation effect observed at the non-constant pre-exponential factor model. First the parameters of the pyrolysis step will be taken into account. Wójtowicz et al. studied tobaccos by TGA-FTIR and obtained E_0 and σ values in the range of 152 - 296 and 1 - 40 kJ/mol, respectively, on the evolution of volatile products during tobacco pyrolysis.[6] De Jong et al. obtained similar ranges for biomasses in a TGA-FTIR study.[36] Yi et al. published 116 pairs of E_0 and σ data on the evolution

of volatile products during tobacco pyrolysis that fell in the range of 128 - 296 and 1 - 40 kJ/mol, respectively.[9] The values of Table 4 of the present work (E_0=186 kJ/mol and $17 \leq \sigma \leq 27$ kJ/mol) are within these intervals. For a closer look one can consider that the DTG curves represent the sum of the mass loss rates of the formed volatiles. Accordingly an E_0 parameter of a DTG curve is expected to be close to the weighted mean of the E_0 values of the formed volatile species. For these purpose we calculated $\overline{E_0}$ averages using the yields of the given species as weight factors from the data of the articles cited above.[6,9,36] This procedure yielded $\overline{E_0}$ values between 157 and 178 kJ/mol for tobaccos[6,9] and 171 – 177 kJ/mol for biomasses.[36]

As mentioned in Section 2.1, the tobacco samples of the present work were studied in inert atmosphere by TGA-MS.[12] The evaluation of the mass spectrometric intensities resulted in similar ranges of E_0 and σ values as the TGA-FTIR studies cited above. The corresponding DTG curves were modeled by four DAEM reactions assuming four pseudocomponents. (Here a pseudocomponent is the totality of those decomposing species which can be described by the same reaction kinetic parameters in the given model.) The pseudocomponents contributed to the overall mass loss by different c quantities. One can form the weighted mean of E_0 using these c values as weights. In this way $\overline{E_0}$ values between 207 and 225 kJ/mol are obtained for the various parameter sets published in the article.[12] These values are higher than the corresponding E_0=186 kJ/mol value in Table 4 of the present work. The difference can be due to the effect of the oxygen: the combustion reaction starts to dominate around 400°C in the present work while the decomposition reactions lasted to higher temperatures in inert atmosphere, accordingly the model described a wider temperature range in inert atmosphere.

The combustion kinetics of biomass chars was excessively reviewed by Di Blasi in 2009.[13] Table 3 of that work surveys the corresponding kinetic parameters. The activation energy values vary between 71 and 229 kJ/mol, while the reaction order with respect to the oxygen concentration is between 0.5 and 1. Table 4 of the present article exhibits E_{char} values between 209 and 213 kJ/mol with $\nu \cong 0.4$. Accordingly the present E_{char} value is near to the higher end of the literature range. ν, however, is lower than the values compiled by Di Blasi. Note that care was taken to ensure a true kinetic regime in the present work: low sample masses were spread in thin layers, the heating rates were not high and the formed CO and CO_2 were quickly swept away from the combusting samples. Accordingly the relatively low ν value cannot be due to diffusion control or to reversible reactions. A Langmuir–Hinshelwood kinetics is not probably for biomass chars under the present conditions.[13]The comparison of the results to the literature data is frequently problematic due to the different experimental conditions and evaluation methods. However, Di Blasi's survey contained, among others, a work of Várhegyi et al. on the combustion of corncob charcoals.[14] This work was based on the simultaneous least squares evaluation of 8 – 12 experiments and the experimental conditions were very similar to those of the present article. Still the activation energies varied between 88 and 152 kJ/mol and all but one ν values lied in the range of 0.53 – 0.91. Note that the present work describes the behavior of complex biomass-type samples by simplified, two-step models. A huge number of chemical reactions are described approximately by

a DAEM devolatilization followed by the burn-off of the forming char. The high E_{char} and low ν values suggest that the division to two reaction steps is only approximate. The border between the devolatilization and the char burn-off reactions is probably not so sharp in the reality. The char burn-off reaction of the present article probably approximates devolatilization reactions, too, which have a low (theoretically zero) reaction order with respect to the oxygen concentration. Similarly, the devolatilization above 400°C has probably higher activation energy than the char burn-off itself; hence the inclusion of some devolatilization increases the overall activation energy of the char burn-off reaction of the present work. Note that the TGA-MS experiments on the same samples in inert atmosphere resulted in activation energies above 250 kJ/mol in the temperature domain of our combustion step[12] while the majority of the char combustion studies reviewed by Di Blasi[13] resulted in activation energies below the 209 – 213 kJ/mol range of E_{char} in the present work.

3. Conclusions

The thermal decomposition and combustion of a Virginia and a Burley tobacco blends was studied at slow heating programs, under well defined conditions. Particularly low sample masses were employed to avoid the self-heating of the samples due to the huge reaction heat of the combustion. The chemical composition of the samples differed markedly.

A combustion model was proposed that consisted of a devolatilization reaction and a successive combustion of the forming char. The devolatilization step was described by a distributed activation energy model (DAEM). The combustion of the forming char was described by two models. The first was first order with respect to the amount of char. The second contained an approximate formula that described the dependence of the combustion on the sample conversion empirically. The dependence of the char combustion on the oxygen concentration was described by a power function. The combustion of the volatiles was not treated in the present work. (It cannot be measured by TGA.) The modeling was based on the simultaneous evaluation of 30 TGA experiments on 2 tobacco blends, 3 oxygen concentrations, two linear heating programs, and two heating programs with isothermal sections. The models gave reasonable description for all of these experiments.

All model variants treated in the paper was evaluated in two ways:

(i) by the separate evaluation of experiments on a given sample (i.e. on series of 15 experiments)

(ii) by the simultaneous experiments of the 30 experiments.

In the later case part of the parameters were assumed to have common values for the two samples. This approach emphasized the similarities in the combustion properties of the tobaccos. Besides, the mathematical condition of the evaluation is also better in this way: the mean number of the unknowns determined from an experiment was only 0.4 – 0.6 in the model variants tested in the paper while the fit remained practically the same as in the separate evaluation of the samples. Some of the parameters evaluated in this way showed only negligible dependence on the model variant or on the sample. The mean activation energy of the

devolatilization was found to be around 184 kJ/mol, the activation energy of the char burn-off was about 211 kJ/mol, and the reaction order with respect to oxygen concentration was around 0.42.

The model variants tested in the paper gave similar fit values; the improvement of the overall fit by introducing more model parameters does not appear to be important from a practical point of view. Nevertheless, they revealed details about the combustion and modeling. The empirical model of the char burn-off indicated a marked dependence of the reactivity on the conversion of sample due to the formation and growth of the pores and their changing accessibility.

The assumption of a constant A in a wide domain of E looks somehow unrealistic; one should expect some dependence of A on E. On the other hand a distribution of the activation energy can approximate a wide range of differences between the reacting species. These aspects were analyzed by assuming a linear dependence between E and log A. It was found that this type of dependence can reasonably be approximated by the proper adjustment of the parameters of a DAEM with constant pre-exponential factor.

Supporting Information Available: Figures illustrating the evaluation of 30 experiments at the model variants treated in the paper. This material is available free of charge via the Internet at http://pubs.acs.org.

NOMENCLATURE

α reacted fraction of the sample (dimensionless)

β parameter expressing the dependence of the pre-exponential factor on the activation energy (kJ^{-1} mol)

ν reaction order with respect of oxygen concentration

A pre-exponential factor (s^{-1})

A_0 pre-exponential factor in a DAEM. If A depends on E then $A_0 = A(E_0)$. (s^{-1})

C_{O_2} V/V concentration of the ambient oxygen (dimensionless)

E activation energy (kJ/mol)

E_0 mean activation energy in a distributed activation energy model (kJ/mol)

fit_N a measure of the fit calculated for a group of N experiments by equations 1 - 2 (%)

h_k height of an experimental curve (s^{-1})

m normalized sample mass (dimensionless)

N number of experiments in a given calculation

N_k number of evaluated data on the kth experimental curve

R gas constant (8.3143$\times$10^{-3} kJ mol^{-1} K^{-1})

σ width parameter (variance) of Gaussian distribution (kJ/mol)

S_N least squares sum for N experiments (dimensionless)

t time (s)

T temperature (°C, K)

Subscripts:

i   digitized point on an experimental curve

k   experiment

ur   unreacted sample

REFERENCES

(1) Burton, H.; Burdick, D. Thermal decomposition of tobacco I. - Thermogravimetric Analysis, *Tobacco Science* **1967**, *11*, 180-185.

(2) Baker, R. R. The kinetics of tobacco pyrolysis, *Thermochim. Acta* **1976**, 17, 29-63.

(3) Muramatsu, M.; S. Umemura, S.; Okada, T. A mathematical model of evaporation-pyrolysis processes inside a naturally smouldering cigarette, *Combust. Flame* **1979**, *36*, 245 - 262.

(4) Burnham, A. K.; Braun, R. L. Global kinetic analysis of complex materials. *Energy Fuels* **1999**, *13*, 1-22.

(5) Avni, E.; Coughlin, R.W.; Solomon P.R., King H.H. Mathematical modelling of lignin pyrolysis. *Fuel* **1985**, *64* 1495-1501.

(6) Wójtowicz, M. A.; Bassilakis, R.; Smith, W. W.; Chen, Y.; Carangelo, R. M. Modeling the evolution of volatile species during tobacco pyrolysis. *J. Anal. Appl. Pyrolysis*, **2003**, *66*, 235-261.

(7) Yi, S-C.; Hajaligol, M. R. Product distribution from the pyrolysis modeling of tobacco particles. *J. Anal. Appl. Pyrolysis*, **2003**, *66*, 217-234.

(8) Rostami, A. A.; Hajaligol, M.R.; Wrenn, S. E. A biomass pyrolysis sub-model for CFD applications. *Fuel* **2004**, *83*, 1519–25.

(9) Yi, S-C.; Hajaligol, M. R.; Jeong, S. H. The prediction of the effects of tobacco type on smoke composition from the pyrolysis modeling of tobacco shreds. *J. Anal. Appl. Pyrolysis*, **2005**, *74*, 181-192.

(10) Saidi, M. S.; Hajaligol, M. R.; Rasouli, F. Numerical simulation of a burning cigarette during puffing. *J. Anal. Appl. Pyrolysis* **2004**, *72*, 141-152.

(11) Becidan, M.; Várhegyi, G.; Hustad, J. E.; Skreiberg, Ø. Thermal decomposition of biomass wastes. A kinetic study. *Ind. Eng. Chem. Res.* **2007**, *46*, 2428 - 2437.

(12) Várhegyi, G.; Czégény, Z.; Jakab, E.; McAdam, K.; Liu, C. Tobacco pyrolysis. Kinetic evaluation of thermogravimetric – mass spectrometric experiments. *J. Anal. Appl. Pyrolysis* **2009**, *86*, 310-322.

(13) Di Blasi, C. Combustion and gasification rates of lignocellulosic chars. *Progr. Energy Combust. Sci.* **2009**, *35*, 121-140.

(14) Várhegyi, G.; Mészáros, E.; Antal, M. J., Jr.; Bourke, J.; Jakab, E. Combustion kinetics of corncob charcoal and partially demineralized corncob charcoal in the kinetic regime. *Ind. Eng. Chem. Res.* **2006**, *45,* 4962-4970.

(15) Eaton, A. M.; Smoot, L. D.; Hill, S. C.; Eatough, C. N. Components, formulations, solutions, evaluation, and application of comprehensive combustion models. *Progr. Energy Combust. Sci.* **1999**, *25*, 387-436.

(16) Czégény, Z.; Blazsó, M.; Várhegyi, G.; Jakab, E.; Liu, C.; Nappi, L. Formation of selected toxicants from tobacco under different pyrolysis conditions, *J. Anal. Appl. Pyrolysis* **2009**, *85*, 47-53.

(17) Várhegyi, G. Aims and methods in non-isothermal reaction kinetics. *J. Anal. Appl. Pyrolysis* **2007**, *79*, 278-288.

(18) Várhegyi, G.; Szabó, P.; Antal, M. J., Jr. Kinetics of charcoal devolatilization. *Energy Fuels* **2002**, *16*, 724-731.

(19) Várhegyi, G.; Till, F. Computer processing of thermogravimetric - mass spectrometric and high pressure thermogravimetric data. Part 1. Smoothing and differentiation. *Thermochim. Acta* **1999**, *329*, 141-145.

(20) Várhegyi, G.; Chen, H.; Godoy, S. Thermal decomposition of wheat, oat, barley and *Brassica carinata* straws. A kinetic study. *Energy Fuels* **2009**, *23*, 646-652.

(21) Donskoi, E.; McElwain, D. L. S. Optimization of coal pyrolysis modeling. *Combust. Flame* **2000**, *122*, 359-367.

(22) IMSL Fortran Library User's Guide, MATH/LIBRARY Volume 1, 2003, Visual Numerics Inc, Houston, Texas 77042.

(23) Várhegyi, G. Integration of the rate constant and linearization of the kinetic equations in nonisothermal reaction kinetics. *Thermochim. Acta* **1978**, *25*, 201-207.

(24) Press, W. H.; Flannery, B. P.; Teukolsky, S. A.; Vetterling, W. T. *Numerical Recipes. The Art of Scientific Computing*. 2nd ed., Cambridge University Press, Cambridge (U.K.), 1992.   (Online Internet edition: http://www.nrbook.com/a/bookfpdf.php .)

(25) Kolda, T. G.; Lewis, R. M.; Torczon, V. Optimization by direct search: New perspectives on some classical and modern methods. *SIAM Rev.* **2003**, 45, 385-482.

(26) Bhatia; S. K; Perlmutter, D. D. A random pore model for fluid–solid reactions: I. Isothermal kinetic control. *AIChE J.* **1980**, *26*, 379-386.

(27) Gavalas, G. R. A random capillary model with application to char gasification at chemically controlled rates. *AIChE J.* **1980**, *26*, 577-585.

(28) Reyes, S.; Jensen, K. F. Percolation concepts in modeling of gas-solid reactions. I. Application to char gasification in the kinetic regime. *Chem. Eng. Sci.* **1986**, *41*, 333-340.

(29) Tseng, H. P.; Edgar, T. F. The change of the physical-properties of coal char during reaction. *Fuel* **1989**, *68*, 114-119.

(30) Várhegyi, G.; Szabó, P.; Jakab, E.; Till, F.; Richard J-R. Mathematical Modeling of Char Reactivity in Ar-O_2 and CO_2-O_2 Mixtures. *Energy Fuels* **1996**, *10*, 1208-1214.

(31) Várhegyi, G.; Pöppl, L.; Földvári, I. Kinetics of the oxidation of bismuth tellurite, Bi_2TeO_5: Empirical model and least squares evaluation strategies to obtain reliable kinetic information. *Thermochim. Acta* **2003**, *399*, 225-239.

(32) Miura, K., A New and Simple Method to Estimate f(E) and k_0(E) in the Distributed Activation Energy Model from Three Sets of Experiment. *Energy Fuels* **1995**, 9, 302-307.

(33) Miura, K.; Maki, T. Simple Method for Estimating f(E) and k_0(E) in the Distributed Activation Energy Model. *Energy Fuels* **1998**, 12, 5, 864-869.

(34) Sonobe, T.; Worasuwannarak, N. Kinetic analyses of biomass pyrolysis using the distributed activation energy model. *Fuel* **2008**, 87, 414-421.

(35) Hashimoto, K.; Miura, K.; Watanabe, T. Kinetics of thermal regeneration reaction of activated carbons used in waste water treatment. *AIChE J*. **1982**, 28, 737-746.

(36) de Jong, W; Pirone, A; Wojtowicz, M. A. Pyrolysis of Miscanthus Gigenteus and wood pellets: TG-FTIR analysis and reaction kinetics. *Fuel,* **2003**, *82*, 1139-1147